

Negatively charged Ir(III) cyclometalated complexes containing a chelating bis-tetrazolato ligand: Synthesis, photophysics and study of reactivity with electrophiles.

Valentina Fiorini,^{a*} Stefano Zacchini,^a Paolo Raiteri,^{b,c} Rita Mazzoni,^a Valerio Zanotti,^a Massimiliano Massi^{b*} and Stefano Stagni^{a,*}

^a Department of Industrial Chemistry "Toso Montanari", University of Bologna, Viale Risorgimento 4, I-40136 Bologna, Italy

^b Department of Chemistry, Curtin University, GPO Box U 1987, Perth, Australia, 6845

^c Curtin Institute for Computation, Curtin University, GPO Box U 1987, Perth, Australia, 6845

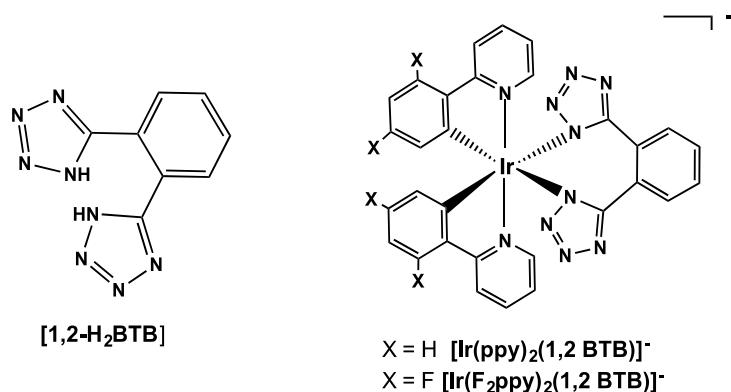
Abstract

The bis-tetrazolate dianion [1,2 BTB]²⁻, which is the deprotonated form of 1,2 bis - (1H tetrazol-5-yl)benzene [1,2-H₂BTB], is for the first time exploited as the ancillary N^N ligand for negatively charged [Ir(C^N)₂(N^N)]⁻ type complexes, where C^N is represented by cyclometalated 2-phenylpyridine (ppy) or 2-(2,4-difluorophenyl)pyridine (F₂ppy). The new Ir(III) complexes [Ir(ppy)₂(1,2 BTB)]⁻ and [Ir(F₂ppy)₂(1,2 BTB)]⁻ have been fully characterised and the analysis of the X-ray structure of [Ir(ppy)₂(1,2 BTB)]⁻ confirmed the coordination of the [1,2 BTB]²⁻ dianion in a bis chelated fashion through the N-atoms adjacent to each of the tetrazolic carbons. Both of the new anionic Ir(III) complexes displayed phosphorescence in the visible region, with intense sky-blue ($\lambda_{\text{max}} = 460\text{-}490\text{ nm}$) or aqua ($\lambda_{\text{max}} = 490\text{-}520\text{ nm}$) emissions originating from [Ir(F₂ppy)₂(1,2 BTB)]⁻ and [Ir(ppy)₂(1,2 BTB)]⁻, respectively. In comparison with our very recent examples of anionic Ir(III)tetrazolate cyclometalates, the new Ir(III) tris chelate complexes [Ir(F₂ppy)₂(1,2 BTB)]⁻ and [Ir(ppy)₂(1,2 BTB)]⁻, display an improved robustness, allowing the study of their reactivity toward the addition of electrophiles such as H⁺ and CH₃⁺. In all cases, the electrophilic attacks occurred at the coordinated tetrazolate rings, involving the reversible – by a protonation deprotonation mechanism – or permanent – upon addition of a methyl moiety – switching of their global net charge from negative to positive and, in particular, the concomitant variation of their photoluminescence output. The combination of the anionic complexes [Ir(F₂ppy)₂(1,2 BTB)]⁻ or [Ir(ppy)₂(1,2 BTB)]⁻ with a deep red emitting ($\lambda_{\text{max}} = 686\text{ nm}$) cationic Ir(III) tetrazole complex such as [IrTPYZ-Me]⁺, where TPYZ-Me is 2-(2-methyl-2H-tetrazol-5-yl)pyrazine, gave rise to two fully Ir(III)-based soft salts capable of displaying additive and O₂-sensitive emission colours, with an almost pure white light obtained by the appropriate choice of the ionic components.

Introduction

The majority of phosphorescent iridium(III)-based ionic transition metal complexes (Ir-iTMC) are typically represented by cationic species, with the general formula $[(C^{\wedge}N)_2Ir(N^{\wedge}N)]^+$, where $C^{\wedge}N$ represents a cyclometalated ligand and $N^{\wedge}N$ is usually a neutral diimine ligand. In this family of complexes, fine tuning of the emission colour can be readily achieved through modifications of the $C^{\wedge}N$ and/or $N^{\wedge}N$ ligand.¹ More recently, a few examples of anionic Ir-iTMCs have also been reported, demonstrating efficient behaviour as phosphors.² This newer class of negatively charged complexes is based around Ir(III) cyanometalates where the neutral diimine is substituted by two cyanide ligands, such as $[Ir(ppy)_2(CN)_2]^-$ and its fluorinated analogue $[Ir(F_2ppy)_2(CN)_2]^-$ (where ppy and F_2ppy represent 2-phenylpyridine and its fluorinated analogue, respectively). These anionic Ir(III) complexes have been employed as emissive materials for Light Emitting Electrochemical Cells (LEECs) and,³ in combination with photoactive cationic complexes, for the formation of luminescent ion pairs (often referred also as “soft salts”).⁴ We have recently expanded the area of anionic Ir(III) complexes with the report of the sky-blue emitting $[Ir(ppy)_2(N_4C-R)_2]^-$ and aqua emitting $[Ir(F_2ppy)_2(N_4C-R)_2]^-$ species, where the two cyano ligands are substituted by the tetrazolate moieties N_4C-R^- (with R representing a phenyl or 4-cyanophenyl substituent). These anionic species have been used in conjunction with red-emitting cationic Ir(III) tetrazole complexes for the formation of soft salts capable of white light emission.⁵ Moving beyond these promising results, we wanted to further investigate the chemistry of anionic Ir(III) tetrazolate complexes with respect to their reactivity toward electrophilic additions. In fact, we have previously shown how the photoluminescent properties of tetrazolato species of Re(I), cationic Ir(III), and Pt(II) could be reversibly or irreversibly tuned by addition of electrophilic reagents to the metal-coordinated tetrazolato ring.⁶ Unfortunately, both $[Ir(ppy)_2(N_4C-R)_2]^-$ and $[Ir(F_2ppy)_2(N_4C-R)_2]^-$ complexes displayed pronounced lability of the tetrazolato ligands in the presence of electrophiles such as CH_3^+ or H^+ . Therefore, to further continue our studies and determine the reactivity and luminescent switching of anionic Ir(III) tetrazolato species, we attempted to prepare a more inert complex by tethering the two tetrazolato rings into a phenyl moiety. To this extent, we herein report the synthesis, together with the spectroscopic, structural and photophysical characterisation of two new $[Ir(ppy)_2(N^{\wedge}N)]^-$ and $[Ir(F_2ppy)_2(N^{\wedge}N)]^-$ type complexes where $N^{\wedge}N$ is a dianionic bis-tetrazolate, such as the fully deprotonated form of 1,2 bis - (1*H* tetrazol-5-yl)benzene (1,2 BTB) (Scheme 1). Furthermore, the new anionic Ir(III) complexes have been investigated with

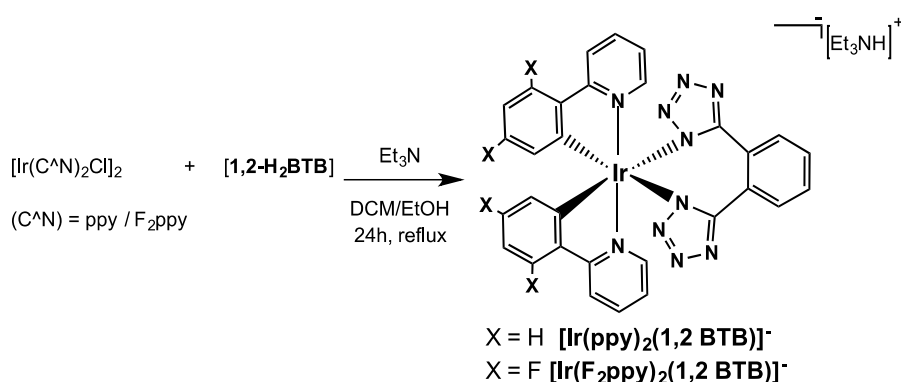
respect to their reactivity versus methyl triflate and triflic acid. Lastly, they have been exploited for the synthesis of soft salts in conjunction with a deep-red cationic Ir(III) tetrazole emitter.



Scheme 1. Ligand, complexes and relative acronyms used in this work.

Results and discussion.

The 1,2-H₂BTB ligand was obtained in good yield by 1,3 dipolar cyclisation of the azide anion (N₃⁻) onto 1,2-dicyanobenzene. Furthermore, the targeted Ir(III) anionic complexes were prepared according to our previously published procedure (Scheme 2),⁵ involving the reaction of the chloro-bridged Ir(III) dimer, [Ir(C^N)₂Ir(μ-Cl)]₂ or [Ir(F₂ppy)₂Ir(μ-Cl)]₂, with a 2.5 molar excess of 1,2-H₂BTB in the presence of an equimolar amount of triethylamine (NEt₃). In all cases, after 24 hours at reflux temperature, the addition of diethyl ether to the crude mixtures caused the precipitation of the desired saline compounds. Conveniently, the products were simply filtered and did not require any further purification.



Scheme 2: Synthetic procedure for the [Ir(C^N)₂(N^N)]⁻ type complexes.

The formation of the desired anionic complexes, which were isolated as their triethylammonium [TEAH]⁺ salts, was initially deduced by Electron Spray Ionisation Mass Spectrometry (ESI-MS), which provided *m/z* signals congruent with the expected anions (ESI, Figures S1-2). Single crystals

suitable for X-ray diffraction could be obtained for $[\text{Ir}(\text{ppy})_2(\text{N}^{\wedge}\text{N})]^-$ (Figure 1 and Table 1, ESI Table S1), revealing how the coordination of the bis-tetrazolate anion $[\text{1,2 BTB}]^{2-}$ to the Ir(III) metal centre effectively occurred in a chelating fashion through the N-1 nitrogen atoms (N(1) and N(5) according to crystallographic numbering in figure 1) of each tetrazolate ring. Effectively, this binding mode describes a seven-membered ($-\text{IrNC}_4\text{N}-$) coordination ring. Because of its chelating coordination, the $[\text{1,2 BTB}]^{2-}$ ligand is not planar, with the two tetrazolate rings forming an angle of 71.8° between their least squares planes, whereas the angles formed between the least squares plane of each tetrazolate ring and the benzene ring are 37.8° and 51.1° , respectively. A similar coordination has been previously observed in the case of Tl(I), Cd(II) and Cu(II) derivatives of the same $[\text{1,2 BTB}]^{2-}$ anion.⁷ Overall, the Ir(III) centre adopts a distorted octahedral coordination geometry with *cis*-metalated phenyl carbon donors and *trans* pyridine nitrogen donors, as was previously found in other complexes containing analogous cyclometalated ligands.^{6c,e} The Ir-N (tetrazolate) distances [$2.157(6)$ and $2.176(6)$ Å] are longer than Ir-N (phenylpyridine) [$2.067(7)$ and $2.058(6)$ Å] because of the *trans* influence of the strongly σ -donating metalated carbon atoms. Intermolecular H-bonding is present involving the N(31)-H(31) group of the $[\text{HNEt}_3]^+$ cation as donor and the N(8) atom of the $[\text{Ir}(\text{ppy})_2(\text{1,2 BTB})]^-$ anion as acceptor [N(31)-H(31) 0.93 Å, H(31)⋯N(8)#1 2.28 Å, N(31)⋯N(8)#1 3.187(15) Å, $\angle\text{N(31)H(31)N(8)\#1}$ 163.3°; symmetry transformations used to generate equivalent atoms #1 $x, y-1, z$].

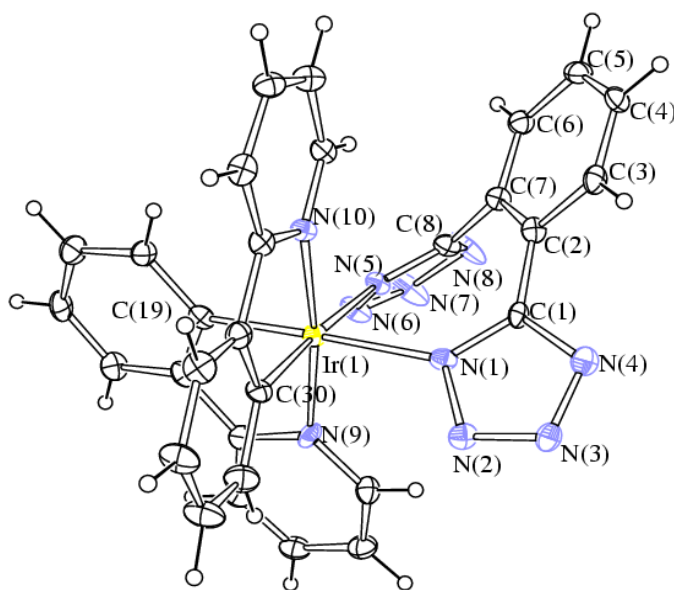
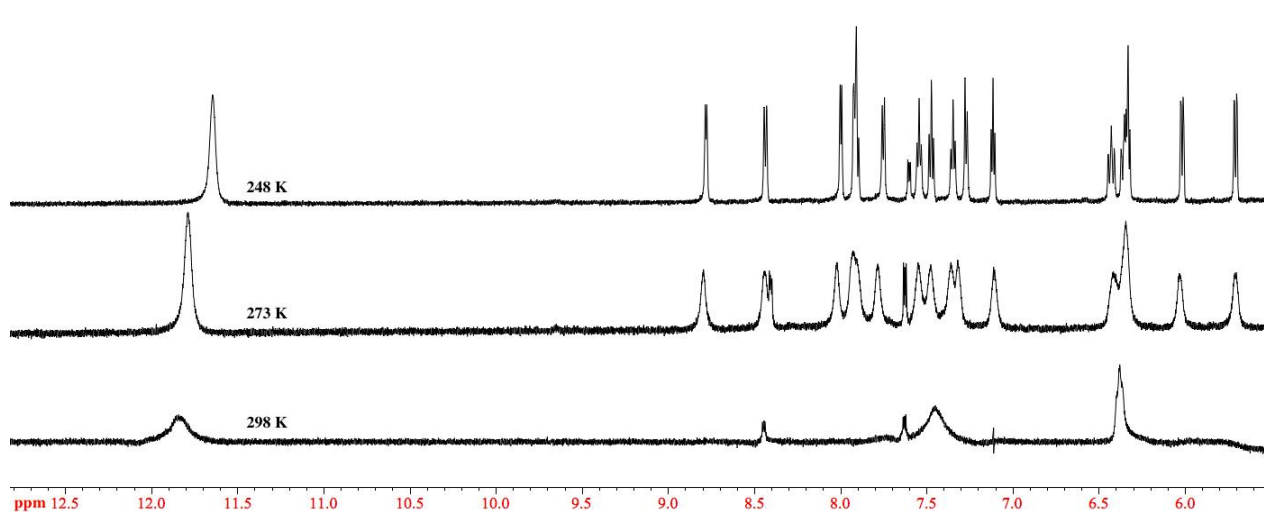


Figure 1: Molecular structure of $[\text{Ir}(\text{ppy})_2(\text{1,2 BTB})]^-$ with key atoms labelled. Displacement ellipsoids are at the 30% probability level.

Table 1: Selected bond lengths (Å) and angles (deg) for $[\text{Ir}(\text{ppy})_2(1,2 \text{ BTB})]^-$.

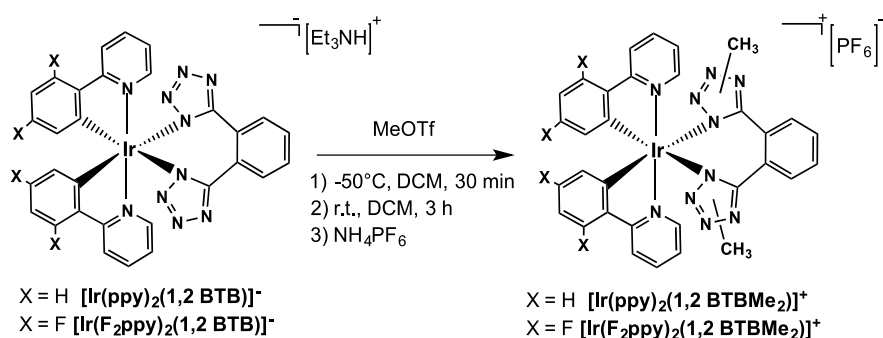
Ir(1)-N(1)	2.157(6)	Ir(1)-N(5)	2.176(6)
Ir(1)-N(9)	2.067(7)	Ir(1)-N(10)	2.058(6)
Ir(1)-C(19)	2.016(8)	Ir(1)-C(30)	2.020(8)
N(1)-N(2)	1.361(9)	N(5)-N(6)	1.357(8)
N(2)-N(3)	1.318(9)	N(6)-N(7)	1.286(10)
N(3)-N(4)	1.340(10)	N(7)-N(8)	1.359(10)
C(1)-N(4)	1.338(10)	C(8)-N(8)	1.343(10)
C(1)-N(1)	1.352(10)	C(8)-N(5)	1.318(10)
C(1)-C(2)	1.467(11)	C(7)-C(8)	1.468(10)
C(2)-C(3)	1.398(10)	C(3)-C(4)	1.398(12)
C(4)-C(5)	1.389(12)	C(5)-C(6)	1.380(11)
C(6)-C(7)	1.389(11)	C(7)-C(2)	1.417(10)
N(1)-Ir(1)-C(19)	176.2(3)	N(5)-Ir(1)-C(30)	176.0(3)
N(9)-Ir(1)-N(10)	172.9(3)	N(1)-Ir(1)-N(5)	85.3(2)
N(9)-Ir(1)-C(19)	80.8(3)	N(10)-Ir(1)-C(30)	80.3(3)

The ^1H and ^{13}C NMR characterisation in CD_2Cl_2 of $[\text{Ir}(\text{ppy})_2(1,2 \text{ BTB})]^-$ and $[\text{Ir}(\text{F}_2\text{ppy})_2(1,2 \text{ BTB})]^-$ required variable temperature (VT) experiments. Well resolved ^1H and ^{13}C NMR spectra could only be obtained at 248 K (Figure 2 and ESI figures S7-9) and displayed a number of signals equal to the total number of hydrogen or carbon atoms in each complex, in agreement with the occurrence of C_s symmetry that can be reasonably explained in consideration of the not coplanar arrangement adopted by the coordinated (1,2 BTB) ligand.

**Figure 2:** Stacking plot of ^1H NMR spectra (CD_2Cl_2 as the solvent, 600 MHz) of $[\text{Ir}(\text{F}_2\text{ppy})_2(1,2 \text{ BTB})]^-$, recorded at 298 K (bottom), 273 K (middle), and 248 K (top).

The likely reason that might account for such a fluxional behaviour might be attributed to the exchange through a ring inversion of the strained seven membered ring (-IrNC₄N-) that is described by the coordinated bis-tetrazolate ligand and the Ir(III) center. The occurrence of a similar mechanism has been described in previous reports dealing with heterocyclic analogues of benzocycloheptene.⁸

The reactivity of [Ir(ppy)₂(1,2 BTB)]⁻ and [Ir(F₂ppy)₂(1,2 BTB)]⁻ was screened with respect to the addition electrophiles such as H⁺ and CH₃⁺. In the former case, the protonation reactions were monitored upon performing emission titrations (*vide infra*), while the preparation of the bis-methylated complexes [Ir(ppy)₂(1,2 BTBMe₂)]⁺ and [Ir(F₂ppy)₂(1,2 BTBMe₂)]⁺ was accomplished through the reaction of the anionic precursors [Ir(ppy)₂(1,2 BTB)]⁻ and [Ir(F₂ppy)₂(1,2 BTB)]⁻ with a slight excess of methyl triflate (Scheme 3). After a metathesis procedure, the cationic complexes were isolated as their hexafluorophosphate salts, as demonstrated by ESI-MS analysis (ESI Figures S3, S4).



Scheme 3: Synthetic procedure for the [Ir(C^N)₂(1,2 BTBMe₂)]⁺ type complexes.

In contrast to what observed for the anionic derivatives, the NMR characterisation of the bis-methylated complexes [Ir(ppy)₂(1,2 BTBMe₂)]⁺ and [Ir(F₂ppy)₂(1,2 BTBMe₂)]⁺ could be accomplished at room temperature, without the need for VT experiments. In particular, each ¹H NMR spectrum displayed pattern of signals congruent with the occurrence of one bis-methylated compound in which the Cs symmetry of the starting anionic complexes is retained, as witnessed by the presence of a number of signals equal to the number of the aromatic hydrogens of the molecules and by the clear splitting of the CH₃ signals into two well spaced peaks having the same integral value (Figure 3 and ESI Figures S11 and S15). Analogous indications came from the analysis of the ¹³C NMR spectra (ESI Figures S12 and S16).

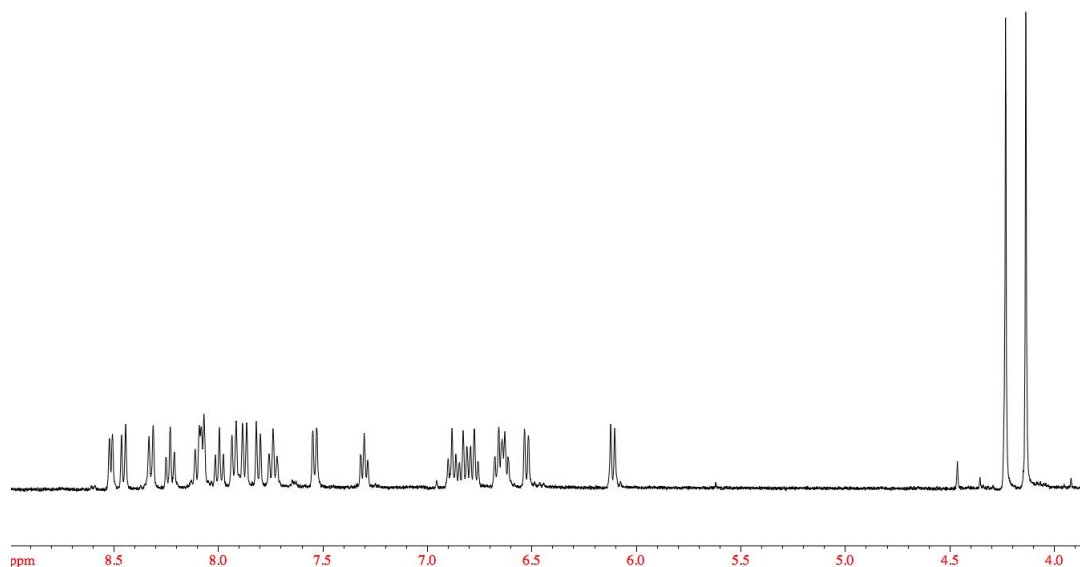


Figure 3: ^1H NMR spectrum of $[\text{Ir}(\text{ppy})_2(1,2 \text{BTBMe}_2)]^+$, Acetone d^6 , 400 MHz, 298 K.

However, the isolation of one single dimethylated product points to the eventual regioselective character of the addition of the methyl group to the coordinated tetrazolato rings, each of which contains three diimine type nitrogens that are in principle prone to electrophilic attack. Even though all the attempts for obtaining crystals suitable for X-ray diffraction of both the cationic complexes were not successful, useful indications about the nature of the bis-methylated isomers could be deduced by means of nuclear Overhauser effect spectroscopy (NOESY). (ESI Figures S13-14 for $[\text{Ir}(\text{ppy})_2(1,2 \text{BTBMe}_2)]^+$ and S17-18 for $[\text{Ir}(\text{F}_2\text{ppy})_2(1,2 \text{BTBMe}_2)]^+$). We can anticipate that the analysis of the results of the NOESY experiments suggested how each methylation likely occurred at the tetrazole nitrogens labelled as N-4 and N-8 in Figure 1, *i.e* in a position adjacent to the tetrazole carbon of each pentatomic ring. More specifically, in the case of the NOESY experiment performed onto the exemplar complex $[\text{Ir}(\text{ppy})_2(1,2 \text{BTBMe}_2)]^+$, the irradiation at the resonance frequency of the $-\text{CH}_3$ hydrogen signal centred at $\delta = 4.13$ ppm, caused the enhancement of the resonance centred at $\delta = 7.80$ ppm, which we assume as the 1,2 BTBMe₂ phenyl hydrogen labelled as H_a in Figure 4. Likewise, the irradiation of the signal centred at $\delta_{\text{H}} = 4.22$ ppm, the one relative to the other CH₃ group of the molecule, resulted in the increase of the signal at $\delta_{\text{H}} = 8.44$ ppm, which is in turn assigned to the 1,2 BTBMe₂ phenyl hydrogen labelled as H_d in Figure 4. Finally, by performing $^1\text{H}-^1\text{H}$ COSY correlation experiments, it was possible to assign the resonances relative to the remaining hydrogens H_b and H_c (see Figure 4), which were found at $\delta_{\text{H}} = 7.97$ and $\delta_{\text{H}} = 8.25$, respectively. Analogous and congruent results were obtained by performing the same experiments (NOESY and $^1\text{H}-^1\text{H}$ COSY) onto the fluorinated complex $[\text{Ir}(\text{F}_2\text{ppy})_2(1,2 \text{BTBMe}_2)]^+$. Also in this case, the methyl moieties are likely bonded at the same positions (N4 and N8, see

Figure 1) as those of the not fluorinated complex $[\text{Ir}(\text{ppy})_2(1,2\text{ BTBMe}_2)]^+$, and the H_a , H_b , H_c and H_d hydrogens (see Figure 4 for labelling) were found to resonate at $\delta_{\text{H}} = 7.81, 8.00, 8.23$ and 8.44 ppm, respectively.

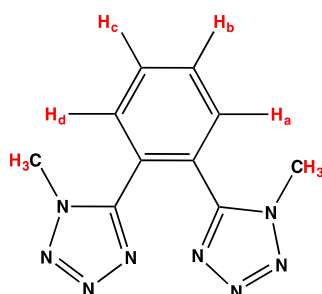


Figure 4: Hydrogen labelling of 1,2 BTBMe₂

Photophysical properties

The photophysical data for $[\text{Ir}(\text{ppy})_2(1,2\text{ BTB})]^-$ and $[\text{Ir}(\text{F}_2\text{ppy})_2(1,2\text{ BTB})]^-$ are listed in table 2. In diluted dichloromethane solutions ($\approx 10^{-5}$ M), the anionic Ir(III) complexes display similar absorption profiles (Figure 5, left), with intense ligand centred (LC) transitions up to 300 nm and metal-to-ligand charge transfer (MLCT) bands tailing off above 350 nm. To confirm the identity of the charge transfer transitions, time-dependent density functional theory (TD-DFT) calculations were used for these complexes (see ESI Figure S70 and Table S2-3). The structures of the complexes were minimised using the implicit solvent model (PCM).⁹ The data indicate that the lower energy band in the spectrum belongs to the HOMO→LUMO+n ($n=0-1$) transition. The HOMO is mainly localised on the Ir(III) centre and phenyl rings of both the ppy ligands. On the other hand, the LUMO and LUMO+1 are localised on both the extended ppy ligands (see Figure 7). The TD-DFT results confirm the MLCT nature of the lowest excited state with admixture of LC character.

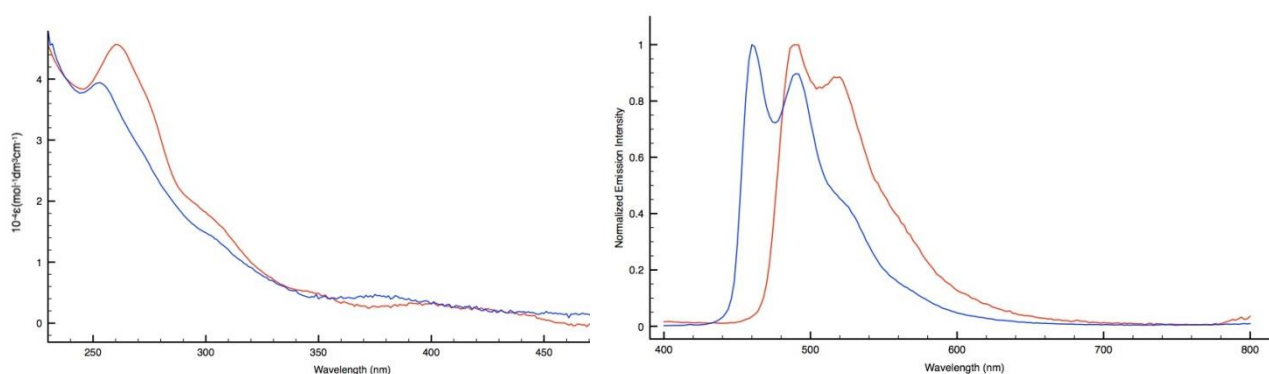


Figure 5: Absorption profiles (left) and normalised emission profiles (right) of $[\text{Ir}(\text{ppy})_2(1,2\text{ BTB})]^-$ (red trace) and $[\text{Ir}(\text{F}_2\text{ppy})_2(1,2\text{ BTB})]^-$ (blue trace).

Table 2: Photophysical properties for $[\text{Ir}(\text{C}^{\wedge}\text{N})_2(1,2\text{ BTB})]^-$, diprotonated $[\text{Ir}(\text{C}^{\wedge}\text{N})_2(1,2\text{ BTBH}_2)]^+$ complexes and the dimethylated $[\text{Ir}(\text{C}^{\wedge}\text{N})_2(1,2\text{ BTBMe}_2)]^+$ complexes.

Complex Solvent: CH_2Cl_2	Absorption λ_{abs} (nm) ($10^{-4} \epsilon$) ($\text{M}^{-1} \text{cm}^{-1}$)	Emission 298 K ^{a, b}					Emission 77K ^c	
		λ (nm)	τ_{Air} (μs)	τ_{Ar} (μs)	Φ_{Air} (%)	Φ_{Ar} (%)	λ (nm)	τ (μs)
$[\text{Ir}(\text{ppy})_2(1,2\text{ BTB})]^-$	261(4.56) 305(1.65) 350(0.49)	488 516	0.10	0.820	2.93	33.3	482 516 562	2.24
$[\text{Ir}(\text{ppy})_2(1,2\text{ BTBMe}_2)]^+$	260 (7.26) 300 (2.81) 386 (0.55)	482 512	0.060	0.106	0.88	2.79	472 506	3.82
$[\text{Ir}(\text{F}_2\text{ppy})_2(1,2\text{ BTB})]^-$	254(2.72) 307(0.89) 370(0.29)	460 490 526	0.120	1.60	2.64	53.0	456 490 524	2.20
$[\text{Ir}(\text{F}_2\text{ppy})_2(1,2\text{ BTBMe}_2)]^+$	248(11.63) 318 (3.13) 370 (1.00)	456 486	0.180	0.254	2.95	6.95	450 482	3.64

^a: “Air” means air equilibrated solutions, “Ar” means deoxygenated solutions under argon atmosphere; ^b: $[\text{Ru}(\text{bpy})_3]\text{Cl}_2/\text{H}_2\text{O}$ was used as reference for quantum yield determinations ($\Phi_r = 0.028$)¹²; ^c: frozen CH_2Cl_2 as the solvent.

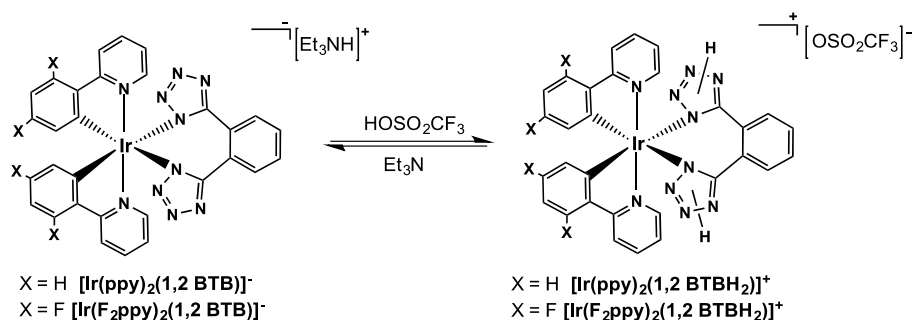
Upon excitation of the MLCT features, the two anionic complexes gave rise to bright sky-blue (λ_{max} ca. 460 and 490 nm) or aqua (λ_{max} ca. 490 and 520 nm) emissions for $[\text{Ir}(\text{F}_2\text{ppy})_2(1,2\text{ BTB})]^-$ and $[\text{Ir}(\text{ppy})_2(1,2\text{ BTB})]^-$, respectively (Figure 5, right). The blue-shift occurring upon replacement of ppy with F_2ppy can be rationalised by a stabilisation of the HOMO localised on the phenyl rings due to the electron-withdrawing nature of the fluoride substituents.

In both cases, the triplet character of the excited state was witnessed by the pronounced oxygen sensitivity that was displayed by the quantum yields (ϕ), which ranged from ca. 0.33 to ca. 0.53 for the deoxygenated solutions of $[\text{Ir}(\text{F}_2\text{ppy})_2(1,2\text{ BTB})]^-$ and $[\text{Ir}(\text{F}_2\text{ppy})_2(1,2\text{ BTB})]^-$, respectively, and the corresponding lifetimes (τ) values (Table 2). In addition, the occurrence of structured emission profiles further confirmed the interplay of $^3\text{LC}/^3\text{MLCT}$ emissive excited states, in agreement with the TD-DFT calculations for these complexes. The lack of rigidochromic effect observable for the small blue-shift on passing from room temperature to 77 K emission suggests a dominant LC character in the composition of the $^3\text{LC}/^3\text{MLCT}$ excited state.

Addition of electrophiles

The addition of electrophiles such as H^+ or CH_3^+ to the anionic complexes $[\text{Ir}(\text{F}_2\text{ppy})_2(1,2\text{ BTB})]^-$ and $[\text{Ir}(\text{ppy})_2(1,2\text{ BTB})]^-$ caused the switching to the corresponding cationic species and induced the

concomitant variation of their photoluminescent features. The occurrence of these effects were first observed in the cases of the protonation reactions (Scheme 4), which were carried out by performing emission titrations in which successive aliquots of triflic acid were added up to two molar equivalents. From the analysis of each titration profile (Figure 6 and ESI Figures S49-54), followed by monitoring changes in the emission plots, it was observed that the sequential protonation of the tetrazolate rings caused significant reduction of the emission intensity. The emission spectra of the cationic products appeared in both cases only slightly blue shifted ($\Delta\lambda = 4-6$ nm) with respect to those of the anionic precursors, whose vibronically structured shape of was maintained throughout the whole titrations. It is worth noting that the protonation reactions described herein share the same reversible character that we have reported previously for Ir(III), Re(I) and Ru(II)-tetrazolato complexes, whose luminescence properties could be reversibly modulated by a protonation-deprotonation mechanism.^{6c} Indeed, the addition of two molar equivalents of a relative weak base such as triethylamine (Et_3N) to the bis-protonated complexes $[\text{Ir}(\text{ppy})_2(1,2\text{ BTBH}_2)]^+$ and $[\text{Ir}(\text{F}_2\text{ppy})_2(1,2\text{ BTBH}_2)]^+$ restored the corresponding anionic precursors and their intense emission profiles (Table 2).



Scheme 4: Reversible protonation reaction of $[\text{Ir}(\text{C}^{\text{N}})_2(1,2\text{ BTB})]^-$ type complexes

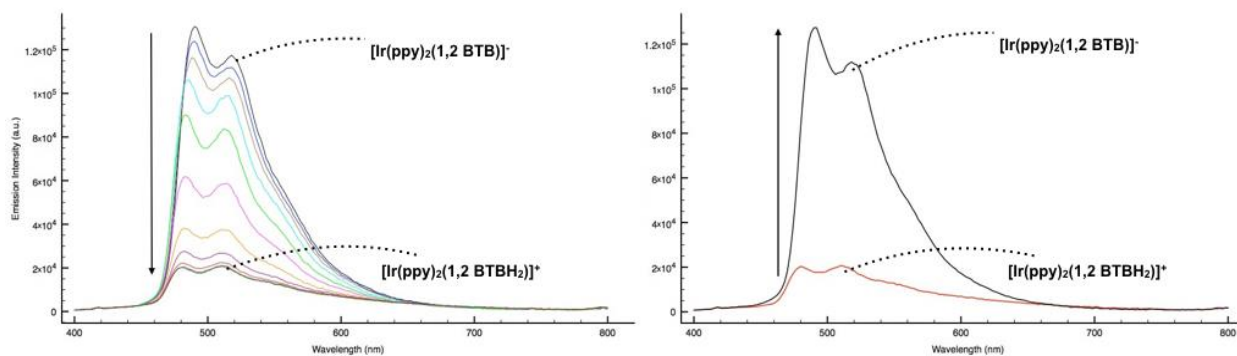


Figure 6: Left: Emission titration of $[\text{Ir}(\text{ppy})_2(1,2\text{ BTB})]^-$ with $110\mu\text{L}$ of HOSO_2CF_3 $0,005$ M in CH_2Cl_2 . Right: Back Titration with Et_3N showing the reversible modulation of the emission intensity between the protonated $[\text{Ir}(\text{ppy})_2(1,2\text{ BTBH}_2)]^+$ and $[\text{Ir}(\text{ppy})_2(1,2\text{ BTB})]^-$.

The photoluminescence behaviour that was observed when the anionic complexes $[\text{Ir}(\text{ppy})_2(1,2\text{ BTB})]^-$ and $[\text{Ir}(\text{F}_2\text{ppy})_2(1,2\text{ BTB})]^-$ were irreversibly transformed into the dimethylated complexes $[\text{Ir}(\text{ppy})_2(1,2\text{ BTBMe}_2)]^+$ and $[\text{Ir}(\text{F}_2\text{ppy})_2(1,2\text{ BTBMe}_2)]^+$, respectively, followed a trend analogous to that observed upon performing the protonation reactions. In particular, as the emission profiles of the dimethylated species were found almost exactly superimposable to those of the diprotonated analogues. It was possible to determine that the addition of electrophiles such as H^+ or CH_3^+ to the starting anionic complexes did not involve appreciable change in the colour of their sky-blue (for $[\text{Ir}(\text{F}_2\text{ppy})_2(1,2\text{ BTB})]^-$) or aqua (in the case of $[\text{Ir}(\text{ppy})_2(1,2\text{ BTB})]^-$) emissions, but concomitantly caused the reduction of the emission quantum yields to *ca.* one tenth of the initial values (Table 2 and ESI, Figures S37-48). Congruently with the analysis of TDDFT calculations (see further on), the occurrence of such particular behaviour, suggests that the protonated $[1,2\text{ BTBH}_2]$ or methylated $[1,2\text{ BTBMe}_2]$ ligands might play a not negligible role in determining the composition of the emissive excited states. In particular, such a pronounced intervention of non-radiative processes might be explained by considering the reduction of the sigma donor character of the dianionic bis-tetrazolate ligand $[(1,2\text{ BTB})]^{2-}$ that takes place upon its transformation into its neutral and protonated $[1,2\text{ BTBH}_2]$ or methylated $[1,2\text{ BTBMe}_2]$ derivative, likely resulting in the weakening of the Ir(III)-N(tetrazole) bond strength.

In line with what emerged from NOESY experiments, the TD-DFT analysis relative to the cationic complexes $[\text{Ir}(\text{ppy})_2(1,2\text{ BTBMe}_2)]^+$ and $[\text{Ir}(\text{F}_2\text{ppy})_2(1,2\text{ BTBMe}_2)]^+$ was carried out by assuming that methylation occurred at the N-4 and N-8 (see Figure 1 for labelling) positions of both tetrazole rings. Similarly to their anionic precursors $[\text{Ir}(\text{ppy})_2(1,2\text{ BTB})]^-$ and $[\text{Ir}(\text{F}_2\text{ppy})_2(1,2\text{ BTB})]^-$, the low energy band of the bis methylated cationic complexes is again ascribed to the HOMO \rightarrow LUMO+n (n=0-1) transition, with the HOMO localised on the Ir(III) centre and phenyl rings of the ppy or F_2ppy cyclometalating ligands. Contrastingly, the LUMO and LUMO+1 of $[\text{Ir}(\text{ppy})_2(1,2\text{ BTBMe}_2)]^+$ and $[\text{Ir}(\text{F}_2\text{ppy})_2(1,2\text{ BTBMe}_2)]^+$ were no longer localised only on the ppy or F_2ppy ligands, but a significant contribution of the phenyl ring of the bis-tetrazole ligand $[1,2\text{ BTBMe}_2]$ was observed in the composition of the LUMO of each of the bis-methylated complexes $[\text{Ir}(\text{ppy})_2(1,2\text{ BTBMe}_2)]^+$ and $[\text{Ir}(\text{F}_2\text{ppy})_2(1,2\text{ BTBMe}_2)]^+$ (Figure 7 and Table 3, ESI Table S2-5). This computational evidence might provide an explanation of how the addition of electrophiles to the anionic precursors can determine the modification of the emission performances of the product cationic complexes.

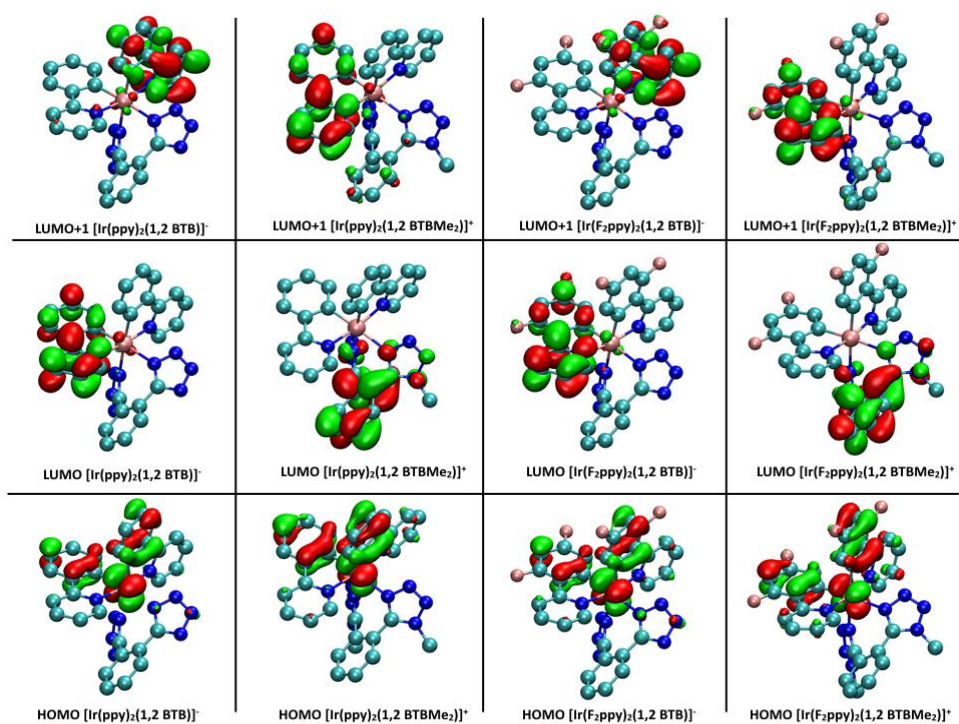


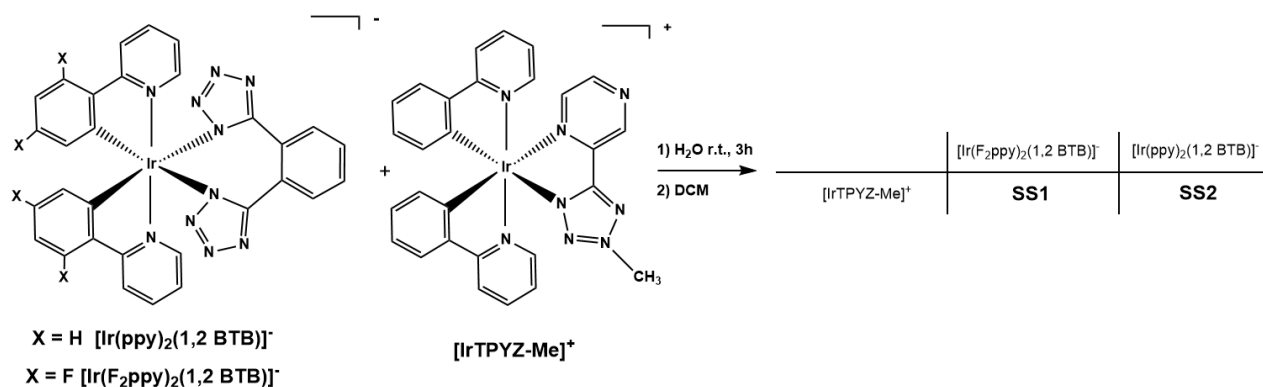
Figure 7: Localisation of the HOMO, LUMO, and LUMO+1 orbitals for the anionic and cationic Ir(III) complexes.

Table 3: Low energy absorption transitions obtained from the TD-DFT calculations for anionic and cationic Ir(III) complexes. For brevity we report here only the transitions with character greater than 10%, while the whole list is reported in the ESI (Table S2-5).

Complex	Wavelength (nm)	Intensity (a.u.)	Transition	Character (%)
[Ir(ppy) ₂ (1,2 BTB)] ⁻	341.45	0.184	HOMO -> LUMO	84.9
	331.95	0.062	HOMO -> LUMO+1	84.8
	286.38	0.096	HOMO-4 -> LUMO	17.0
			HOMO-2 -> LUMO	45.0
HOMO -> LUMO+2			15.7	
281.09	0.193	HOMO -> LUMO+2	62.7	
[Ir(ppy) ₂ (1,2 BTBMe ₂)] ⁺	329.58	0.207	HOMO -> LUMO+1	66.4
			HOMO -> LUMO+2	13.7
	320.67	0.076	HOMO -> LUMO+2	61.7
	276.16	0.285	HOMO-2 -> LUMO+1	30.0
HOMO-1 -> LUMO+1			31.4	
273.50	0.070	HOMO --> LUMO+4	56.4	
[Ir(F ₂ ppy) ₂ (1,2 BTB)] ⁻	322.42	0.177	HOMO -> LUMO	80.1
	314.42	0.066	HOMO -> LUMO+1	81.1
	278.89	0.161	HOMO-2 -> LUMO	11.9
			HOMO-1 -> LUMO	55.6
	269.14	0.072	HOMO-4 -> LUMO	47.1
HOMO-3 -> LUMO			10.3	
HOMO-2 -> LUMO			14.3	
[Ir(F ₂ ppy) ₂ (1,2 BTBMe ₂)] ⁺	312.50	0.218	HOMO-1 -> LUMO+1	14.3
			HOMO -> LUMO+1	62.7
			HOMO -> LUMO+2	11.8
	305.21	0.103	HOMO-1 -> LUMO+2	12.5
HOMO -> LUMO+2			64.7	
284.84	0.003	HOMO -> LUMO	89.3	
272.90	0.323	HOMO-2 -> LUMO+1	42.4	
		HOMO-1 -> LUMO+1	25.4	

Soft salts

The photophysical behaviour of the anionic Ir(III) complexes $[\text{Ir}(\text{F}_2\text{ppy})_2(1,2\text{ BTB})]^-$ and $[\text{Ir}(\text{ppy})_2(1,2\text{ BTB})]^-$ was also investigated upon their combination with the tetrazole-based cationic complex $[\text{IrTPYZ-Me}]^+$ to form the fully Ir(III) soft salts SS1 and SS2, respectively (Scheme 5).



Scheme 5: Synthetic procedure for Ir(III) soft salts and relative acronyms.

As we reported previously,⁵ the cation $[\text{IrTPYZ-Me}]^+$ displays much different luminescent features with respect to those of the anionic complexes. In particular, under the same experimental conditions (10^{-5} M in CH_2Cl_2 , 298 K, $\lambda_{\text{exc}} = 370$ nm) as those used for the anionic species $[\text{Ir}(\text{F}_2\text{ppy})_2(1,2\text{ BTB})]^-$ and $[\text{Ir}(\text{ppy})_2(1,2\text{ BTB})]^-$, the cationic complex $[\text{IrTPYZ-Me}]^+$ displays red ($\lambda_{\text{max}} = 686$ nm) phosphorescence that originates from MLCT-type excited states, as witnessed by the broad and unstructured emission which undergoes to a significant blue shift on passing to 77 K (Table 4 and ESI Figures S51-53).

Upon excitation ($\lambda_{\text{exc}} = 370$ nm) of the corresponding air-equilibrated and diluted (10^{-5} M) dichloromethane solutions, the photoluminescence spectra of the newly obtained soft salts again display the emission of both the anionic and cationic counterparts (Figure 8), with lifetimes parameters that do not differ appreciably with respect to those of the individual mononuclear complexes (Table 5). In these conditions, the emission colours of the soft salts SS1 and SS2 (see ESI, Figures S58-61 for SS1, S62-69 for SS2) represent the rough sum of the ionic components, with an almost white emission originating from the soft salt SS1, in which the red emitting cation $[\text{IrTPYZ-Me}]^+$ is paired to the blue sky emitter $[\text{Ir}(\text{F}_2\text{ppy})_2(1,2\text{ BTB})]^-$. In perfect agreement with our previous results,⁵ the deoxygenated dichloromethane solutions of the soft salts SS1 and SS2 showed the predominant emission (blue for SS1 and green for SS2, Table 4 and Figure 8; right, for 1931 C.I.E coordinates) of the anionic complexes. This feature can be explained in consideration of

the different variation of quantum yield experienced by the anionic and cationic iridium complexes upon degassing, which is related to their diverse excited state lifetime.

Table 4: Photophysical properties for Ir(III) tetrazolate soft salts.

Complex	Absorption λ_{abs} (nm) $(10^{-4} \epsilon) (\text{M}^{-1} \text{cm}^{-1})$	Emission 298 K ^{a, b}					Emission 77K ^c		C.I.E	
		λ (nm)	$\tau_{\text{Air}}(\mu\text{s})$	$\tau_{\text{Ar}}(\mu\text{s})$	$\Phi_{\text{Air}}(\%)$	$\Phi_{\text{Ar}}(\%)$	λ (nm)	$\tau(\mu\text{s})$	ox	deox
SS1 – [Ir(F ₂ ppy) ₂ (1,2 BTB)] [IrTPYZ-Me] ⁺	259(5.6)	464	0.12	0.65						
	312(2.0)	490	0.12	0.68	2.9	16.6	574	3.7	X 0.339	X 0.243
	380(0.8)	674	0.07	0.08					Y 0.363	Y 0.385
SS2 – [Ir(ppy) ₂ (1,2 BTB)] ⁻ [IrTPYZ-Me] ⁺	262(7.0)	490	0.08	1.30						
	307(2.9)	522	0.07	1.20	3.1	22.4	568	3.9	X 0.430	X 0.267
	379(1.0)	670	0.10	0.10					Y 0.463	Y 0.539
[IrTPYZ-Me]⁺	265(6.8)	686	0.09	0.10	2.7	3.6	582	4.5	-	-
	327(1.7)									
	377(1.1)									

^a: “Air” means air equilibrated solutions, “Ar” means deoxygenated solutions under argon atmosphere; ^b: [Ru(bpy)₃]Cl₂/H₂O was used as reference for quantum yield determinations ($\Phi_r = 0.028$)¹²; ^c: frozen CH₂Cl₂ as the solvent.

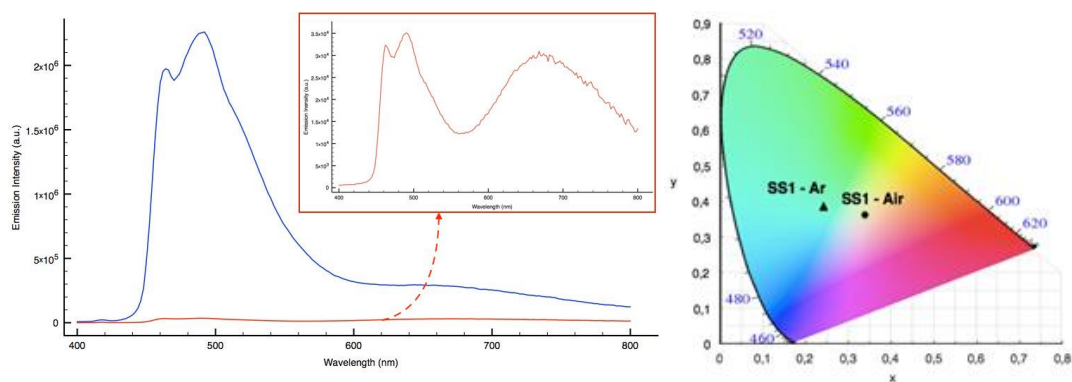


Figure 8: Emission profile (Left) of SS1 10⁻⁵M, CH₂Cl₂, 298 K: Air equilibrated solution, red line/box, Deoxygenated solution blue line; 1931 C.I.E coordinates (Right, Ar – deoxygenated solution, Air – Air equilibrated solution).

Conclusions

In conclusion, we successfully synthesised two new negatively charged Ir(III) tris-chelate complexes with general formulae $[\text{Ir}(\text{ppy})_2(\text{N}^{\wedge}\text{N})]^-$ and $[\text{Ir}(\text{F}_2\text{ppy})_2(\text{N}^{\wedge}\text{N})]^-$, where a bis-tetrazolate dianion such as the deprotonated form of 1,2 bis - (1*H* tetrazol-5-yl)benzene [1,2- H_2BTB] is used for the first time as the ancillary $\text{N}^{\wedge}\text{N}$ ligand. These complexes have been designed in order to provide an upgraded and more robust version of the first examples of brightly luminescent tetrazolate based anionic Ir(III) cyclometalates $[\text{Ir}(\text{F}_2\text{ppy})_2(\text{N}_4\text{C-R})_2]^-$ and $[\text{Ir}(\text{ppy})_2(\text{N}_4\text{C-R})_2]^-$, in which the negative charge was brought by the coordination of two 5-aryl tetrazolato ligands $[\text{N}_4\text{C-R}]^-$. The tethering of two tetrazolate moieties into the bis chelating ligand $[\text{1,2 BTB}]^{2-}$ did not affect the luminescent performances of the resulting anionic complexes $[\text{Ir}(\text{F}_2\text{ppy})_2(\text{1,2 BTB})]^-$ and $[\text{Ir}(\text{ppy})_2(\text{1,2 BTB})]^-$, which also displayed sky-blue or aqua phosphorescent emissions, respectively, with quantum yield values up to 53%, as for deoxygenated solutions of $[\text{Ir}(\text{F}_2\text{ppy})_2(\text{1,2 BTB})]^-$. Further studies about the use of the new anionic complexes as emissive dopants for LEECs (Light Emitting Electrochemical Cells) are currently underway. The improved robustness of the new Ir(III) tris chelate complexes $[\text{Ir}(\text{F}_2\text{ppy})_2(\text{1,2 BTB})]^-$ and $[\text{Ir}(\text{ppy})_2(\text{1,2 BTB})]^-$, allowed the systematic study of their reactivity toward the addition of electrophiles such as H^+ and CH_3^+ . In particular, we could determine that the addition of such electrophiles to the negatively charged $[\text{Ir}(\text{F}_2\text{ppy})_2(\text{1,2 BTB})]^-$ and $[\text{Ir}(\text{ppy})_2(\text{1,2 BTB})]^-$ caused the reversible - by a protonation-deprotonation mechanism - or permanent, as in the case of methylation reaction, switching to their cationic analogues, which displayed the same emission colours of the starting anionic derivatives even if with emission quantum yields significantly reduced.

Importantly, the new anionic complexes $[\text{Ir}(\text{F}_2\text{ppy})_2(\text{1,2 BTB})]^-$ and $[\text{Ir}(\text{ppy})_2(\text{1,2 BTB})]^-$ were combined with a deep red emitting and cationic Ir(III) tetrazole complex to form a new set of Ir(III) based soft salts capable of displaying O_2 -sensitive and properly additive synthesis of the emission colours. Following this behaviour, it was possible to obtain the emission of white light by the appropriate choice of the ionic components.

Experimental Section

General considerations. All the reagents and solvents were obtained commercially (e.g. Aldrich) and used as received without any further purification, unless otherwise specified. All the reactions were carried out under an argon atmosphere following Schlenk protocols. Where required, the purification of the Ir(III) complexes was performed via column chromatography with the use of neutral alumina as the stationary phase. ESI-mass spectra were recorded using a Waters ZQ-4000 instrument (ESI-MS, acetonitrile as the solvent). Nuclear magnetic resonance spectra (consisting of ^1H and ^{13}C) were always recorded using a Varian Mercury Plus 600 (^1H , 599.7; ^{13}C , 150.8 MHz.) for variable temperature experiments (from -50°C to $+25^\circ\text{C}$) and a Varian Mercury Plus 400 (^1H , 399.9; ^{13}C , 101.0 MHz.) for room temperature experiments. ^1H and ^{13}C chemical shifts were referenced to residual solvent resonances. For hydrogen labelling, refer to Figure 4.

Photophysics. Absorption spectra were recorded at room temperature using a Perkin Elmer Lambda 35 UV/vis spectrometer. Uncorrected steady-state emission and excitation spectra were recorded on an Edinburgh FLSP920 spectrometer equipped with a 450 W xenon arc lamp, double excitation and single emission monochromators, and a Peltier-cooled Hamamatsu R928P photomultiplier tube (185–850 nm). Emission and excitation spectra were acquired with a cut-off filter (395 nm) and corrected for source intensity (lamp and grating) and emission spectral response (detector and grating) by a calibration curve supplied with the instrument. The wavelengths for the emission and excitation spectra were determined using the absorption maxima of the MLCT transition bands (emission spectra) and at the maxima of the emission bands (excitation spectra). Quantum yields (Φ) were determined using the optically dilute method by Crosby and Demas¹⁰ at excitation wavelength obtained from absorption spectra on a wavelength scale [nm] and compared to the reference emitter by the following equation:¹¹

$$\phi_s = \phi_r \left[\frac{A_r(\lambda_r)}{A_s(\lambda_s)} \right] \left[\frac{I_r(\lambda_r)}{I_s(\lambda_s)} \right] \left[\frac{n_s^2}{n_r^2} \right] \left[\frac{D_s}{D_r} \right]$$

where A is the absorbance at the excitation wavelength (λ), I is the intensity of the excitation light at the excitation wavelength (λ), n is the refractive index of the solvent, D is the integrated intensity of the luminescence, and Φ is the quantum yield. The subscripts r and s refer to the reference and the sample, respectively. A stock solution with an absorbance > 0.1 was prepared, then two dilutions were obtained with dilution factors of 20 and 10, resulting in absorbances of

about 0.02 and 0.08 respectively. The Lambert-Beer law was assumed to remain linear at the concentrations of the solutions. The degassed measurements were obtained after the solutions were bubbled for 10 minutes under Ar atmosphere, using a septa-sealed quartz cell. Air-equilibrated $[\text{Ru}(\text{bpy})_3]\text{Cl}_2/\text{H}_2\text{O}$ solution ($\Phi = 0.028$)¹² was used as reference. The quantum yield determinations were performed at identical excitation wavelengths for the sample and the reference, therefore deleting the $I(\lambda_r)/I(\lambda_s)$ term in the equation. Emission lifetimes (τ) were determined with the single photon counting technique (TCSPC) with the same Edinburgh FLSP920 spectrometer using pulsed picosecond LED (ELED 360, fwhm < 800 ps) as the excitation source, with repetition rates between 1 kHz and 1 MHz, and the above-mentioned R928P PMT as detector. The goodness of fit was assessed by minimizing the reduced χ^2 function and by visual inspection of the weighted residuals. To record the 77 K luminescence spectra, the samples were put in quartz tubes (2 mm diameter) and inserted in a special quartz dewar filled with liquid nitrogen. The solvent used in the preparation of the solutions for the photophysical investigations was of spectrometric grade. Experimental uncertainties are estimated to be $\pm 8\%$ for lifetime determinations, $\pm 20\%$ for quantum yields, and ± 2 nm and ± 5 nm for absorption and emission peaks, respectively.

TD-DFT calculations

Time-dependent density functional theory calculations were performed with GAUSSIAN 09.¹³ Prior to these calculations, the structures were relaxed at the CAM-B3LYP level of theory.¹⁴ The Ir atoms were treated with the Stuttgart-Dresden effective core potential,¹⁵ the Pople 6-311G** basis set was used for C, H, F and N atoms, and the effect of the solvent was mimicked with the PCM solvation model,⁹ with parameters adequate for dichloromethane.

Ligand synthesis

Warning! Tetrazole derivatives are used as components for explosive mixtures.¹⁶ In this lab, the reactions described here were only run on a few grams scale and no problems were encountered. However, great caution should be exercised when handling or heating compounds of this type. Following the general method reported by Finnegan and coworkers,¹⁷ the ligand [1,2 H₂-BTB] was obtained in almost quantitative yield, while [H-TPYZ], 2-(1H-tetrazol-5-yl)pyrazine, was synthesized according to the procedure reported by Koguro and coworkers.¹⁸

[1,2 H₂-BTB] ¹H-NMR (400 MHz, DMSO *d*⁶) δ (ppm) = 7.91 – 7.89 (m, 2H), 7.81 – 7.78 (m, 2H). [H-TPYZ] ¹H-NMR (400 MHz, DMSO-*d*⁶) δ (ppm) = 9.39 (m, 1H); 8.87 (m, 2H).

General Procedure for the Preparation of the Anionic [Ir(C[^]N)₂(N[^]N)]⁻ Type Complexes

In a 50 mL two neck round bottom flask equipped with a stirring bar, 1 equiv of dichlorobridged iridium dimer and 2.5 equiv of [1,2 H₂-BTB] were added to a 3:1 solution of CH₂Cl₂/EtOH. Then, 2.5 equiv of Et₃N were added, and the resulting mixture was stirred at reflux for 24 h. The solution was restored to r.t. and a small amount of Et₂O (5mL) was added to the mother liquor and the respective products, bright yellow solids, precipitated from the solution, collected by filtration and washed with Et₂O (2x10 mL).

[Ir(ppy)₂(1,2 BTB)]⁻ Y = 76.5%, 0.058 g ¹H-NMR (600 MHz), CD₂Cl₂, 248K, δ (ppm) = 11.45 (s, br, 1H), 8.73 (s, br, 1H, H_d), 8.02 (d, 1H, *J*_{H-H} = 8.39 Hz, H_c), 7.84 (m, 2H, H_b and ppy), 7.71 (d, 1H, *J*_{H-H} = 7.79 Hz, H_a), 7.54 (m, 2H), 7.38 – 7.34 (m, 2H), 7.21 – 7.05 (m, 3H), 6.84 – 6.82 (m, 1H), 6.79 – 6.77 (m, 1H), 6.74 – 6.72 (m, 1H), 6.62 – 6.60 (m, 1H), 6.49 (d, 1H, *J*_{H-H} = 7.79 Hz), 6.23 (m, 1H), 6.12 (d, 1H, *J*_{H-H} = 7.79 Hz). ¹³C-NMR (150.8 MHz), CD₂Cl₂, 248K, δ (ppm) = 168.60, 168.06, 151.33, 150.70, 145.10, 144.08, 137.30, 136.53, 132.53, 131.63, 131.20, 131.15, 129.95, 128.90, 128.63. ESI-MS (*m/z*) CH₃CN, [M]⁻ = 712; [M]⁺ = 102 (Et₃NH). Crystals suitable for X-ray analysis (identified as [Ir(ppy)₂(1,2 BTB)][Et₃NH]) were obtained by slow diffusion of diethyl ether into a solution of the complex in dichloromethane. Anal. Calcd. for C₃₆H₃₆N₁₁Ir (814.96): C 53.06, H 4.45, N 18.91. Found: C 53.07, H 4.47, N 18.90 %

[Ir(F₂ppy)₂(1,2 BTB)]⁻ Y = 59%, 0.043 g ¹H-NMR (600 MHz), CD₂Cl₂, 248K, δ (ppm) = 11.64 (s, br, 1H), 8.78 (d, 1H, *J*_{H-H} = 5.99 Hz, H_d), 8.44 (d, 1H, *J*_{H-H} = 8.99 Hz, H_c), 8.00 (d, 1H, *J*_{H-H} = 4.79 Hz, H_b), 7.92 – 7.89 (m, 2H, H_a and F₂ppy), 7.75 (m, 1H), 7.55 – 7.53 (m, 1H), 7.48 – 7.46 (m, 1H), 7.36 – 7.33 (m, 1H), 7.27 (m, 1H), 7.12 – 7.10 (m, 1H), 6.44 – 6.37 (m, 1H), 6.35 – 6.32 (m, 1H), 6.02 – 6.00 (m, 1H), 5.71 – 5.69 (m, 1H). ¹³C-NMR (150.8 MHz), CD₂Cl₂, 248K, δ (ppm) = 165.42, 164.76, 163.13, 161.91, 161.46, 160.93, 157.74, 157.21, 151.48, 151.14, 137.98, 137.37, 131.63, 131.15, 130.74, 129.57, 129.54, 129.46, 129.20, 128.64, 128.43, 128.21, 128.14, 123.92, 122.51, 122.08, 121.85, 120.16, 114.63, 113.18. ESI-MS (*m/z*) [M]⁻ = 784; [M]⁺ = 102 (Et₃NH) Anal. Calcd. for C₃₆H₃₂N₁₁F₄Ir (886.92): C 48.75, H 3.64, N 17.37. Found: C 48.70, H 3.66, N 17.40 %

General Procedure for the Preparation of the Cationic [Ir(C[^]N)₂(N[^]N)]⁺ Complex

[IrTPYZ-Me]⁺[PF₆]⁻ was obtained according to a previously reported procedure.⁵

[IrTPYZ-Me]⁺ Y = 61.5%, 0.038 g ¹H-NMR (Acetone-*d*⁶, 400 MHz) δ (ppm) = 9.76 (s, 1H), 8.99 (m, 1H), 8.26 (d, 2H, *J*_{H-H} = 8.8 Hz), 8.11 (s, 1H), 8.02 – 7.95 (m, 3H), 7.91 – 7.85 (m, 3H), 7.15 – 6.85 (m, 6H), 6.32 – 6.27 (m, 2H), 4.61 (s, 3H). ¹³C-NMR (CD₃CN, 100 MHz) δ (ppm) = 168.48, 168.18, 166.55 (Ct), 152.62, 151.90, 151.52, 147.39, 146.72, 146.38, 145.74, 145.69, 145.30, 141.25, 140.51, 133.14, 132.77, 131.93, 131.36, 126.41, 125.98, 125.26, 125.11, 124.80, 124.38, 121.51, 121.28, 118.81, 43.47. **ESI-MS** (*m/z*): [M⁺] = 663 [M⁻] = 145 (PF₆). Anal. Calcd. for C₂₈H₂₂N₈F₆PIr (807.71): C 41.63, H 2.75, N 13.87. Found: C 41.65, H 2.77, N 13.86 %

General Procedure for the Preparation of Ir(III) Soft Salts

Ir(III) soft salts SS1 and SS2 were obtained according to our previously reported procedure.⁵ The desired anionic tetrazolate complex [Ir(F₂ppy)₂(1,2 BTB)]⁻ or [Ir(ppy)₂(1,2 BTB)]⁻ and the cationic tetrazole complex [IrTPYZ-Me]⁺ were combined in 1/1 stoichiometric ratio in 15 mL of water. The reaction mixture was stirred for 3 h at room temperature and then extracted with dichloromethane. The organic phase was washed repeatedly with water in order to get rid of triethylammonium and hexafluorophosphate salts. SS1: **ESI-MS** (*m/z*): [M⁺] = 663; [M⁻] = 785; SS2: **ESI-MS** (*m/z*): [M⁺] = 663; [M⁻] = 713. For both SS1 and SS2, the ¹H NMR spectra (CD₃CN, 298 K) displayed well resolved signals only for the cationic counterpart [IrTPYZ-Me]⁺, see ESI, Figures S15 and S16. Anal. Calcd. for SS1 [C₅₈H₃₈N₁₈F₄Ir₂•2H₂O (1483.49)]: C 46.96, H 2.85, N 17.00. Found: C 49.88, H 2.79, N 17.08%; Anal. Calcd. for SS2 [C₅₈H₄₂N₁₈Ir₂•2H₂O (1411.53)]: C 49.35, H 3.28, N 17.86. Found: C 49.28, H 3.25, N 17.98%

General Procedure for the preparation of [Ir(C[^]N)₂(N[^]NMe₂)]⁺- type complexes

Methylation of [Ir(ppy)₂(1,2 BTB)]⁻ and [Ir(F₂ppy)₂(1,2 BTB)]⁻ was carried out according to a previously reported procedure.⁵ The complex [Ir(C[^]N)₂(1,2 BTB)]⁻ (1 eq.) was added to dichloromethane and the mixture was allowed to cool down by immersion into an ethanol/liquid nitrogen cold bath. Then, methyl trifluoromethanesulfonate (2.1 eq., solution in dichloromethane 0.179 M) was added. The reaction was stirred under nitrogen for 30 minutes while being kept in the cold bath, then allowed to warm up to room temperature and stirred for 3 hours. Anion exchange was carried out by adding an excess of NH₄PF₆ in water to the solution and stirring for 20 minutes. The product was then extracted using dichloromethane (3 × 10 mL) and the organic components were combined and dried over anhydrous MgSO₄.

[Ir(ppy)₂(1,2 BTBMe₂)]⁺ Y = 31.7%, 0.021 g ¹H-NMR (400 MHz), Acetone-*d*⁶, 298K, δ (ppm) = 8.51 (d, 1H, *J*_{H-H} = 5.59 Hz), 8.44 (m, 1H, H_d), 8.32 (m, 1H), 8.25-8.19 (m, 1H, H_c), 8.09-8.05 (m, 2H), 8.00-7.96 (m, 1H, H_b), 7.92-7.85 (m, 2H), 7.80-7.78 (m, 1H, H_a), 7.74-7.70 (m, 1H), 7.53-7.51 (m, 1H), 7.30-7.29 (m, 1H), 6.87-6.76 (m, 3H), 6.66-6.61 (m, 2H), 6.52 (d, 1H, *J*_{H-H} = 7.59 Hz), 6.11 (d, 1H, *J*_{H-H} = 7.59 Hz), 4.22 (s, 3H, CH₃), 4.12 (s, 3H, CH₃). ¹³C-NMR (100 MHz), Acetone-*d*⁶, 298K, δ (ppm) = 168.86, 168.09, 154.54 (Ct), 153.74 (Ct), 151.32, 150.28, 146.58, 144.12, 138.54, 137.72, 133.71, 13.19, 132.16, 131.04, 129.12, 128.65, 124.28, 123.66, 122.82, 121.97, 121.92, 121.83, 121.27, 119.25, 118.84, 35.86, 35.63. **ESI-MS** (*m/z*) [M]⁺ = 743; [M]⁻ = 145 (PF₆). Anal. Calcd. for C₃₂H₂₆N₁₀F₆P₁Ir₁ (887.80): C 43.29, H 2.95, N 15.78. Found: C 43.31, H 2.94, N 15.77 %

[Ir(F₂ppy)₂(1,2 BTBMe₂)]⁺ Y = 28.7%, 0.019 g ¹H-NMR (400 MHz), Acetone-*d*⁶, 298K, δ (ppm) = 8.52 (d, 1H, *J*_{H-H} = 8.39 Hz), 8.43-8.41 (m, 2H, H_d and F₂ppy), 8.24-8.17 (m, 3H, H_c and F₂ppy), 8.07 (d, 1H, *J*_{H-H} = 8.39 Hz), 8.00-7.96 (m, 1H, H_b), 7.85-7.80 (m, 2H, H_a and F₂ppy), 7.37-7.34 (m, 1H), 6.73-6.70 (m, 1H), 6.64-6.51 (m, 2H), 5.97-5.94 (m, 1H), 5.64-5.62 (m, 1H), 4.24 (s, 3H, CH₃), 4.14 (s, 3H, CH₃). ¹³C-NMR (100 MHz), Acetone-*d*⁶, 298K, δ (ppm) = 165.72, 165.10, 164.59, 161.93, 160.51, 159.94, 155.56 (Ct), 154.86 (Ct), 152.41, 152.03, 151.97, 151.86, 151.78, 140.61, 139.89, 134.76, 134.32, 133.25, 129.84, 129.11, 123.99, 123.78, 123.36, 122.82, 116.14, 114.23, 99.20, 99.12, 98.85, 98.66, 36.91, 36.72. **ESI-MS** (*m/z*) [M]⁺ = 815; [M]⁻ = 145 (PF₆). Anal. Calcd. for C₃₂H₂₂N₁₀F₁₀P₁Ir₁ (959.76): C 40.05, H 2.31, N 14.59. Found: C 40.00, H 2.30, N 14.61 %

X-ray crystallography.

Crystal data and collection details for [HNEt₃][Ir(ppy)₂(1,2-BTB)] are reported in Table S1, ESI. The diffraction experiments were carried out on a Bruker APEX II diffractometer equipped with a CCD detector and using Mo-Kα radiation. Data were corrected for Lorentz polarization and absorption effects (empirical absorption correction SADABS.¹⁹ Structures were solved by direct methods and refined by full-matrix least-squares based on all data using *F*².²⁰ H-atoms were placed in calculated positions, and refined isotropically using a riding model. All non-hydrogen atoms were refined with anisotropic displacement parameters, a part from disordered atoms. One Et groups of the [HNEt₃]⁺ cation is disordered: this has been split into two positions and refined isotropically using one occupancy factor per disordered group. Similar *U* restraints (SIMU line in SHELXL; s.u. 0.01) were applied to the [HNEt₃]⁺ cation.

CCDC 1486766 for [HNEt₃][Ir(ppy)₂(1,2-BTB)]⁻ contain the supplementary crystallographic data for this paper.

Electronic Supporting Information (ESI) available: NMR (^1H , ^{13}C , NOESY, ^1H - ^1H COSY) and ESI-MS spectra of all the Ir(III) based species. UV-vis absorption, emission spectra recorded at r.t and 77K, plots of the emission titrations, crystallographic data, TD-DFT calculations.

Acknowledgements

The authors wish to thank the Toso Montanari Foundation for financial supporting. P.R. and M.M. would like to thank the Australian Research Council for funding (FT130100463 and FT130100033). This work was also supported by resources provided by National Computational Infrastructure (NCI), which is supported by the Australian Government. The authors also would like to thank Alessandra Petrolì (Università di Bologna) for the NMR acquisitions.

References

- [1] (a) L. Flamigni, A. Barbieri, C. Sabatini, B. Ventura and F. Barigelletti, *Top. Curr. Chem.*, 2007, **281**, 143-203; (b) V. Fernandez-Moreira, F. L. Thorp-Greenwood and M. P. Coogan, *Chem. Commun.*, 2010, **46**, 186–202; (c) Zhang, K. Y.; Lo, K. K.-W. Chemosensing and Diagnostics in *Coordination and Organometallic Chemistry* (Volume **8**) of Comprehensive Inorganic Chemistry II; (d) V. W.-W. Yam, *Ed. Elsevier: Amsterdam*, 2013, 657 – 732 and references cited therein; (e) R. D. Costa, E. Orti, H. J. Bolink, F. Monti, G. Accorsi and N. Armaroli, *Angew. Chem. Int. Ed.*, 2012, **51**, 8178-8211.
- [2] a) M. K. Nazeeruddin R. Humphry-Baker, D. Berner, S. Rivier, L. Zuppiroli and M. Graetzel, *J. Am. Chem. Soc.*, 2003, **125**, 8790-8797; b) D. Di Censo, S. Fantacci, F. De Angelis, C. Klein, N. Evans, K. Kalyanasundaram, H. J. Bolink, M. Gratzel and M. K. Nazeeruddin, *Inorg. Chem.*, 2008, **47**, 980–989.
- [3] H. F. Chen, C. Wu, M. C. Kuo, M. E. Thompson and K. T. Wong, *J. Mater. Chem.*, 2012, **22**, 9556-9561.
- [4] (a) M. Mauro, K. C. Schuermann, R. Prétôt, A. Hafner, P. Mercandelli, A. Sironi and L. De Cola, *Angew. Chem. Int. Ed.*, 2010, **49**, 1222-1226; (b) C. Wu, H. F. Chen, K. T. Wong and M. E. Thompson, *J. Am. Chem. Soc.*, 2010, **132**, 3133-3139; (c) A. Ionescu, E. I. Szerb, Y. J. Yadav, A. M. Talarico, M. Ghedini and N. Godbert, *Dalton Trans.*, 2014, **43**, 784-789; (d) M. Sandroni and E. Zysman-Colman, *Dalton Trans.*, 2014, **43**, 3676-3680; (e) K. N. Swanick, M. Sandroni, Z. Ding and E. Zysman-Colman, *Chemistry – Eur. J.*, 2015, **21**, 7435-7440.
- [5] V. Fiorini, A. D'Ignazio, K. D. M. Magee, M. I. Odgen, M. Massi and S. Stagni, *Dalton Trans.* 2016, **45**, 3256-3259.
- [6] (a) V. Fiorini, A. M. Ranieri, S. Muzzioli, K. D. M. Magee, S. Zacchini, N. Akabar, A. Stefan, M. I. Ogden, M. Massi and S. Stagni; *Dalton Trans.*, 2015, **44**, 20597–20608; (b) M. V. Werrett, G. S. Huff, S. Muzzioli, V. Fiorini, S. Zacchini, B. W. Skelton, A. Maggiore, J. M. Malicka, M. Cocchi, K. C. Gordon, S. Stagni and M. Massi; *Dalton Trans.*, 2015, **44**, 8379–8393; (c) M. V. Werrett, S. Muzzioli, P. J. Wright, A. Palazzi, P. Raiteri, S. Zacchini, M. Massi and S. Stagni; *Inorg. Chem.*, 2014, **53**, 229–243; (d) K. D. M. MaGee, P. J. Wright, S. Muzzioli, C. M. Siedlovskas, P. Raiteri, M. V. Baker, D. H.

Brown, S. Stagni and M. Massi; *Dalton Trans.*, 2013, **42**, 4233–4236. (e) S. Stagni, E. Orselli, A. Palazzi, L. De Cola, S. Zacchini, C. Femoni, M. Marcaccio, F. Paolucci and S. Zanarini, *Inorg. Chem.*, 2007, **46**, 9126–9138.

[7] (a) S. Bhandari, M. F. Mahon, K. C. Molloy, J. S. Palmer and S. F. Sayers, *Dalton Trans.* 2000, 1053; (b) D.-Z. Wang, *Polyhedron* 2012, **35**, 142; (c) Cu X.-H. Huang, T.-L. Sheng, S.-C. Xiang, R.-B. Fu, S.-M. Hu, Y.-M. Li and X.-T. Wu, *Chin. J. Struct. Chem.* 2007, **26**, 161.

[8] A. R. Katritzky Novruz, G. Akhmedov, I. Ghiviriga and R. Maimait; *J. Chem. Soc., Perkin Trans*, 2002, **2**, 1986–1993.

[9] J. Tomasi, B. Mennucci and R. Cammi; *Chem. Rev.*, 2005, **105**, 2999–3094.

[10] G. A. Crosby and J. N. Demas, *J. Phys. Chem.* 1971, **75**, 991–1024.

[11] D. F. Eaton, *Pure Appl. Chem.*, 1988, **60**, 1107–1114.

[12] K. Nakamura, *Bull. Chem. Soc. Jpn.*, 1982, **55**, 2697–2705.

[13] M. J. Frisch, G. W. Trucks, H. B. Schlegel, G. E. Scuseria, M. A. Robb, J. R. Cheeseman, G. Scalmani, V. Barone, B. Mennucci, G. A. Petersson, H. Nakatsuji, M. Caricato, X. Li, H. P. Hratchian, A. F. Izmaylov, J. Bloino, G. Zheng, J. L. Sonnenberg, M. Hada, M. Ehara, K. Toyota, R. Fukuda, J. Hasegawa, M. Ishida, T. Nakajima, Y. Honda, O. Kitao, H. Nakai, T. Vreven, J. A. Montgomery Jr., J. E. Peralta, F. Ogliaro, M. Bearpark, J. J. Heyd, E. Brothers, K. N. Kudin, V. N. Staroverov, R. Kobayashi, J. Normand, K. Raghavachari, A. Rendell, J. C. Burant, S. S. Iyengar, J. Tomasi, M. Cossi, N. Rega, J. M. Millam, M. Klene, J. E. Knox, J. B. Cross, V. Bakken, C. Adamo, J. Jaramillo, R. Gomperts, R. E. Stratmann, O. Yazyev, A. J. Austin, R. Cammi, C. Pomelli, J. W. Ochterski, R. L. Martin, K. Morokuma, V. G. Zakrzewski, G. A. Voth, P. Salvador, J. J. Dannenberg, S. Dapprich, A. D. Daniels, Ö. Farkas, J. B. Foresman, J. V. Ortiz, J. Cioslowski and D. J. Fox, *Gaussian 09, Revision A.02*.

[14] T. Yanai, D. P. Tew and N. C. Handy; *Chem. Phys. Lett.*, 2004, **393**, 51–57.

[15] D. Andrae, U. Haeussermann, M. Dolg, H. Stoll and H. Preuss; *Theor. Chim. Acta*, 1990, **77**, 123–141.

-
- [16] R. N. Butler, Tetrazoles. In *“Comprehensive Heterocyclic Chemistry II”*; Storr, R. C., Ed.; Pergamon Press: Oxford, U.K., 1996; Vol. **4**, 621-678, and references cited therein.
- [17] W. G. Finnegan, R. A. Henry and R. Lofquist; *J. Am. Chem. Soc.*, 1958, **15**, 3908.
- [18] K. Koguro, T. Oga, S. Mitsui and R. Orita, *Synthesis* 1998, 910-914.
- [19] G.M Sheldrick, SADABS, Program for Empirical Absorption Correction, University of Göttingen, Germany, 1996.
- [20] G. M. Sheldrick, SHELX97-Program for the refinement of Crystal Structure, University of Göttingen, Germany, 1997.